

University of Wollongong

Research Online

Faculty of Engineering and Information
Sciences - Papers: Part A

Faculty of Engineering and Information
Sciences

2013

Graphene micro-substrate induced high electron-phonon coupling in MgB₂

W X. Li

University of Wollongong, wenxian@uow.edu.au

X Xu

University of Wollongong, xun@uow.edu.au

K S. B De Silva

University of Wollongong, kaludewa@uow.edu.au

F X. Xiang

University of Wollongong, fx963@uowmail.edu.au

S X. Dou

University of Wollongong, shi@uow.edu.au

Follow this and additional works at: <https://ro.uow.edu.au/eispapers>



Part of the [Engineering Commons](#), and the [Science and Technology Studies Commons](#)

Recommended Citation

Li, W X.; Xu, X; De Silva, K S. B; Xiang, F X.; and Dou, S X., "Graphene micro-substrate induced high electron-phonon coupling in MgB₂" (2013). *Faculty of Engineering and Information Sciences - Papers: Part A*. 352. <https://ro.uow.edu.au/eispapers/352>

Research Online is the open access institutional repository for the University of Wollongong. For further information contact the UOW Library: research-pubs@uow.edu.au

Graphene micro-substrate induced high electron-phonon coupling in MgB₂

Abstract

Electron-phonon coupling strength was studied in graphene-MgB₂ composites to explore the possibilities for a higher superconducting transition temperature (T_c). For the first time in the experimental work on MgB₂, the Raman active E_{2g} mode was split into two parts: a softened mode corresponding to tensile strain and a hardened mode attributed to the carbon substitution effect. The tensile strain effect is suggested to improve T_c of graphene-MgB₂ composites because it increases the electron-phonon coupling strength of MgB₂.

Keywords

phonon, graphene, electron, high, coupling, induced, substrate, micro, mgb2

Disciplines

Engineering | Science and Technology Studies

Publication Details

Li, W. X., Xu, X., De Silva, K. S. B., Xiang, F. X. & Dou, S. X. (2013). Graphene micro-substrate induced high electron-phonon coupling in MgB₂. *IEEE Transactions on Applied Superconductivity*, 23 (3), 1-4.

Graphene micro-substrate induced high electron-phonon coupling in MgB_2

W. X. Li, X. Xu, K. S. B. De Silva, F. X. Xiang, and S. X. Dou

Abstract—Electron-phonon coupling (EPC) strength was studied in graphene- MgB_2 composites to explore the possibilities for a higher superconducting transition temperature (T_c). For the first time in the experimental work on MgB_2 , the Raman active E_{2g} mode was split into two parts: a softened mode corresponding to tensile strain and a hardened mode attributed to the carbon substitution effect. The tensile strain effect is suggested to improve T_c of graphene- MgB_2 composites because it increases the EPC strength of MgB_2 .

Index Terms—Raman spectroscopy, electron-phonon coupling, superconductivity, MgB_2

I. INTRODUCTION

SELF-OPTIMIZATION of intermetallic MgB_2 compound in terms of both electronic structure and phonon dispersion has left only a slim chance for further enhancement in the superconducting transition temperature, T_c , above ~ 39.4 K [1]. Higher T_c of Mg^{10}B_2 and band structure calculations have indicated that MgB_2 is a Bardeen-Cooper-Schrieffer (BCS)-Eliashberg superconductor with two superconducting gaps and strong electron-phonon coupling (EPC): the superconducting bands consist of the strong coupling σ -band and the weakly coupling π -band [2]. The dominant nature of the σ -band is attributed to its coupling with B-B stretch modes, since the boron layer is responsible for the E_{2g} symmetry mode, the only Raman active phonon mode [3]. Chemical substitution and external pressure compress the MgB_2 lattice with a Grüneisen parameter, γ_G , of 2.0–4.0 to stiffen the E_{2g} mode and reduce its contribution to the EPC [4]. Tensile strain has been proved to be effective in increasing the T_c to as high as 41.8 K in MgB_2 thin films on SiC substrates with a softened E_{2g} mode [5]. Substrates with a slightly larger biaxial lattice constant than bulk MgB_2 , such as AlN, GaN, $\text{Al}_x\text{Ga}_{1-x}\text{N}$, and $\text{Mg}_{1-x}\text{Ca}_x\text{B}_2$, have also proven to be effective candidates to induce tensile strain in MgB_2 thin films [6]. Graphene, which has been proved to introduce a strong flux pinning force into MgB_2 [7], is another potential substrate for this purpose. Alternating MgB_2 and graphene layers has also been suggested to expand the

lattice parameters by a factor of 1.1% in bulk MgB_2 [8]. In this work, the T_c behavior was studied, based on the two-gap feature and the phonon dispersion in graphene-added MgB_2 , with the graphene doping level up to 20 wt% via the diffusion method. It was found that the tensile strain effect was the dominant effect in the 5 wt% low graphene added MgB_2 , compensating for the carbon substitution effect, based on the X-ray diffraction (XRD) results. The most exciting result came with the observed softening of the E_{2g} mode in graphene- MgB_2 composites, which might lead to possible higher T_c values in graphene- MgB_2 composites if the processing conditions are optimized. Although tensile strain effects are clearly demonstrated in the composites, judging from the phonon behavior, graphene added samples showed no sign of T_c improvement, due to the strong dominance of carbon substitution and impurity scattering.

II. EXPERIMENTAL SECTION

Graphene- MgB_2 composites were fabricated via a diffusion process using ball-milled crystalline boron powder (0.2 to 2.4 μm , 99.999%), with graphene (micrometer extent, supplied by Prof. J. Stride) added up to 20 wt% in a toluene medium. Then, the vacuum dried powders were mixed and pressed into pellets 13 mm in diameter by 1 mm in thickness. The pellets were sealed in an iron tube filled with Mg powder (-325 mesh 99%) and sintered at 850°C for 10 hrs in a quartz tube furnace with a heating rate of $5^\circ\text{C}/\text{min}$ in high purity argon (Ar 99.9%) flow. Based on their graphene contents of 0, 0.5, 1, 2, 3, 5, 10, and 20 wt%, the samples were denoted as G000, G005, G010, G020, G030, G050, G100, and G200 in the following context, respectively.

All samples were characterized by X-ray diffraction (XRD, D\max-2200), and the crystal structure was refined with the aid of JADE 5.0 software. The microstructures were observed with field emission scanning electron microscopy (SEM, JSM-6700F) and the transmission electron microscopy (TEM: JEOL-2010). The T_c values were deduced from the temperature dependence curves of AC susceptibility, which were measured using a Physical Properties Measurement System (PPMS: Quantum Design). The Raman scattering was measured by a confocal laser Raman spectrometer (Renishaw inVia plus) with a $100\times$ microscope. The 514.5 nm Ar^+ laser was used for excitation, with the laser power maintained at about 20 mW, measured on the laser spot on the samples, in order to avoid laser heating effects on the studied materials. Several spots were selected on the same sample to collect the Raman signals in order to make sure that the results were consistent.

Manuscript received 9 October 2012. This work was supported by the Australian Research Council through a Discovery Project grant (DP0770205).

W. X. Li, X. Xu, K. S. B. De Silva, F. X. Xiang, S. X. Dou are with Institute for Superconducting and Electronic Materials, University of Wollongong, Wollongong, NSW 2522, Australia (S. X. Dou phone: +61-2-42981446; fax: +61-2-42215731; e-mail: wenxian@uow.edu.au).

W. X. Li is also with Solar Energy Technologies, School of Computing, Engineering and Mathematics, University of Western Sydney, Penrith, NSW 2751, Australia. (W. X. Li phone: +61-2-46203552; fax: +61-2-3075; e-mail: w.li@uws.edu.au).

III. RESULTS AND DISCUSSION

According to the XRD patterns, no second phase was found in G000-G030, as shown in the left inset of Fig. 1. A trace of MgB_2C_2 was observed in G050, and the amounts became significant in G100 and G200 due to the high graphene contents. A small amount of MgO can also be found in G100 and G200. The refinement results also show little difference in the length of the c -axis parameter, as shown in Fig. 1. The a -axis shrinkage can be deduced from both the refinement results and obvious shifts of the (1 1 0) planes with graphene addition, as shown in the right inset of Fig. 1. Carbon substitution on the boron sites in the MgB_2 lattice leads to lattice contraction, due to the fact that the length of the C-B bond, 0.172 nm, is shorter than that of the B-B bond, 0.178 nm. Compared with nanocarbon doped MgB_2 [9-11], the lattice parameters estimated from the XRD patterns show weak dependence on the graphene content compared with MgB_2 doped with normal carbon, as shown in Fig. 1. The small variation in the a lattice parameter in the graphene- MgB_2 can be attributed to either the expanding effect of tensile strain or the weak carbon substitution effect, similar with the magnetic processing effect of carbon nano tube doped MgB_2 [12-14].

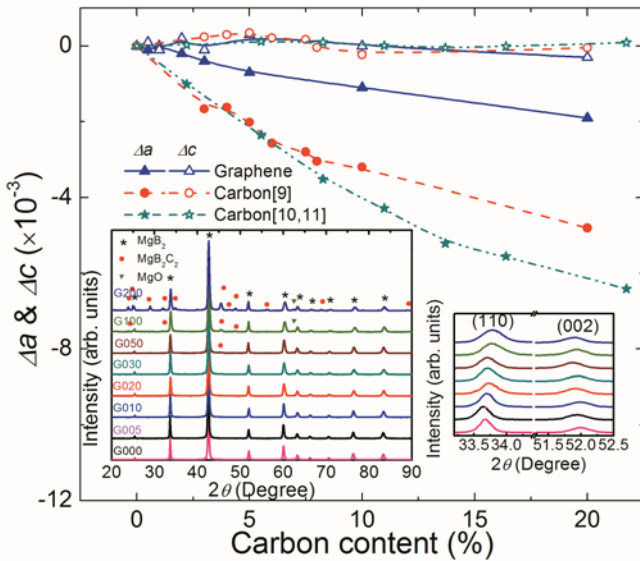


Fig. 1. The effects of graphene addition in MgB_2 on the refined lattice parameters, which are comparable with those of carbon [9-11]. The lattice parameters of pure MgB_2 are $a = 0.3084$ nm and $c = 0.3525$ nm, respectively. The left inset shows the X-ray diffraction patterns of graphene- MgB_2 composites indexed with MgB_2 , MgB_2C_2 , and MgO, and the right inset shows the diffraction peak shift of the (1 1 0) and (0 0 2) planes of MgB_2 .

The magnetic transition temperature, T_c , shows slightly higher values compared with the T_c in nano-carbon doped samples at the same doping levels [9-11]. It should be noted that the T_c dependence on graphene is concave up, which means that T_c depression is restrained by the graphene micro-substrates compared with previous reported work on other forms of carbon, as shown in Fig. 2. The T_c dependences on the lengths of a -axis for different carbon sources are compared in the inset of Fig. 2. It clearly shows that the T_c depends greatly on the lattice parameter for all carbon sources. Figs. 3(a)-3(c) show the SEM images of graphene, G000, and G050. The micrometer extent of graphene is much bigger than the grain sizes of G000 and G050, 200-400nm, which means

that the graphene sheets are big enough acting as micro-substrates for MgB_2 crystals. Figs. 3(d)-3(g) show the TEM and high resolution transmission electron microscopy (HREM) images of G000 and G050. Both the TEM and HREM images of G000 show homogeneous structure with low density of defects. However, G050 has relatively higher density of defects. It should be noted that the order of fringes varies from grain to grain, indicates that the defect is due to highly anisotropic of the interface. Similar fringes have been reported in the MgB_2 where these fringes were induced by tensile stress with dislocations [5]. As the graphene- MgB_2 composites were sintered at 850 °C for 10 hrs, the samples are expected to be well crystalline and contain few defects. The large amount of defects and amorphous phases on the nanoscale are attributed to the residual thermal strain between the graphene and the MgB_2 during cooling process because the thermal expansion coefficient of graphene is very small while that for MgB_2 is large and highly anisotropic. The in-plane lattice parameter, a , is 0.246 nm for graphene, which has a C-C bond length of 0.142 nm, which is much shorter than the a -axis parameter of MgB_2 , 0.3084 nm. The a -axis length would be shrinking due to lattice mismatch if MgB_2 crystals were grown on graphene along the c -axis. However, the mismatch is relaxed due to the weak interlayer coupling, and an expanded MgB_2 lattice is generated in proper supercell structures [8]. It should be noted that such a complex supercell structure is very hard to synthesize by the current solid state reaction method. What we can imagine is that MgB_2 crystals grow on the graphene surfaces, which act as micro-substrates in the polycrystalline composite.

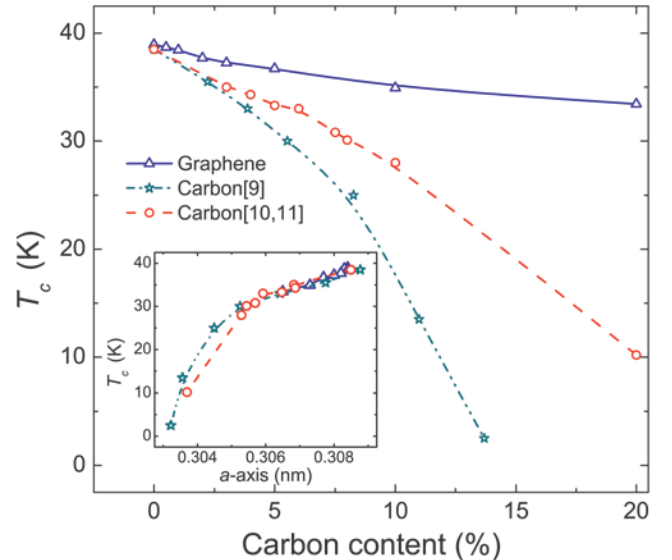


Fig. 2. Comparison of the effects of graphene and carbon addition in MgB_2 on the critical transition temperature [9-11]. The normalized moment dependence on temperature is shown in the inset.

To confirm the effects of tensile strain on the EPC, Raman scattering was employed to examine the phonon properties. Fig. 4(a) shows the typical Raman spectrum of pure MgB_2 , which consists of three broad peaks. The most prominent phonon peak located at lower frequency (ω_2 : centered at ~ 600 cm^{-1}) is assigned to the E_{2g} mode [3],[15]. The other two Raman bands, (ω_1 : centered at 400 cm^{-1} and ω_4 : centered at 730 cm^{-1}) are attributed to the phonon density of states (PDOS) due to disorder [3],[16, 17]. The EPC strength in MgB_2 depends

greatly on the frequency and full width at half maximum (FWHM or Γ) of the E_{2g} mode [18], while the other two modes, especially the ω_4 mode, are responsible for the T_c depression in chemically doped MgB₂ [4]

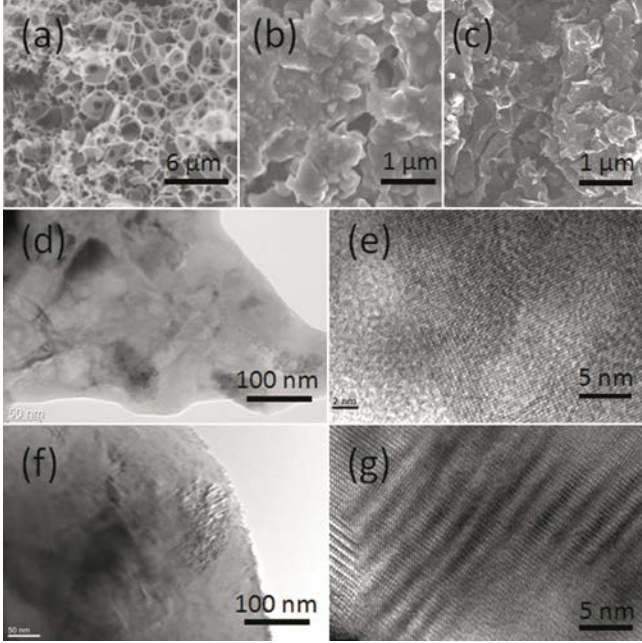


Fig. 3. SEM images of graphene (a), G000 (b), and G050 (c); and TEM and HRTEM images of (d), (e) G000 and (f), (g) G050.

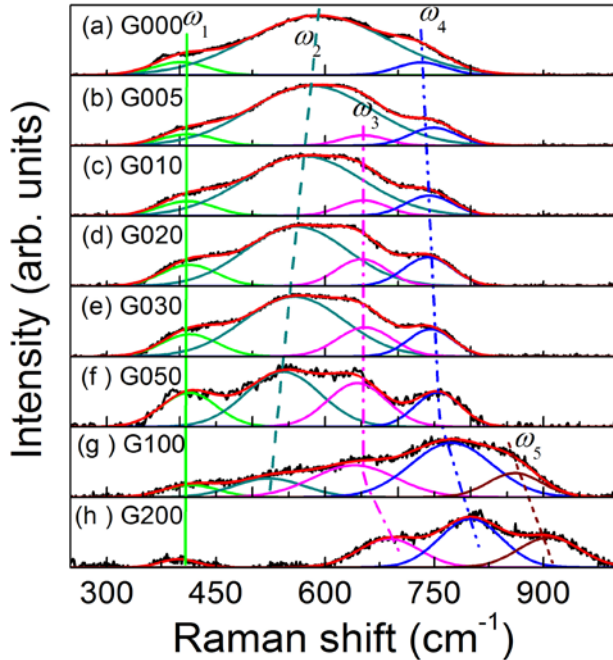


Fig. 4. Influence of graphene content on the Raman spectra of graphene-MgB₂ composites, with measurement at room temperature. The spectra are fitted with ω_1 , ω_2 , ω_3 , and ω_5 , arising from the sampling of the phonon density of states due to disorder, and ω_2 and ω_3 , representing the split E_{2g} mode.

Graphene addition to MgB₂ induces splitting of the E_{2g} mode, resulting in one softened mode (ω_2) and another hardened mode (ω_3). The strong tensile strain stimulates the shift of ω_2 to lower frequency with increasing graphene addition. The softening of the E_{2g} mode was previously observed only in MgB₂-SiC thin films due to tensile-strain-induced bond-stretching, which resulted in a T_c as high as 41.8 K [5]. ω_2 modes are dominant in the low graphene content samples, and no substantial drop in T_c

was observed. This is in agreement with the energy gap behavior, as with carbon substitution induced band filling and interband scattering. According to the McMillan-Allen-Dynes analysis [19, 20], $T_c = \omega e^{-f(\lambda, \hat{\mu})}$, where ω is the phonon frequency, $f(\lambda, \hat{\mu}) = (1 + \lambda) / (\lambda - \hat{\mu})$, where $\hat{\mu}$ is equal to the Coulomb repulsion, μ^* and λ is EPC strength. The EPC due to the σ -band and the bond-stretching mode becomes $\lambda \propto \frac{m^* |D|^2}{M \omega^2}$, where the σ -band effective mass m^* is proportional to the density of states (DOS) of holes in the σ -band at the Fermi level, D is the σ -band deformation potential, and M is the B mass. A change in T_c can arise from any combination of changes in ω , D , m^* , or $\hat{\mu}$. In strained MgB₂, a small deviation in Δa and Δc of the lattice constants results in the variation of λ , $\omega_{E_{2g}}$, μ^* , and T_c . The change in T_c

can be expressed as $\frac{\Delta T_c}{T_c} = \frac{\Delta \omega_{E_{2g}}}{\omega_{E_{2g}}} - \alpha \frac{\Delta \mu^*}{\mu^*} + \beta \frac{\Delta \lambda}{\lambda}$ with

$$\alpha = \frac{1.04(1 + \lambda_0)(1 + 0.62\lambda_0)\mu_0^*}{[\lambda_0(1 - 0.62\mu_0^*) - \mu_0^*]^2}, \quad \beta = \frac{1.04\lambda_0(1 + 0.38\mu_0^*)}{[\lambda_0(1 - 0.62\mu_0^*) - \mu_0^*]^2},$$

and $\frac{\Delta \lambda}{\lambda} = \frac{\Delta N_\sigma(E_F)}{N_\sigma(E_F)} + \frac{2\Delta|D|}{|D|_0} - 2\frac{\Delta \omega_{E_{2g}}}{\omega_{E_{2g}}}$. All variables with

subscript 0 are for strain-free MgB₂. It is clear that the enlarged lattice parameter and low frequency E_{2g} mode induced by tensile strain will surely enhance the EPC of MgB₂. However, the lattice shrinkage and the high frequency ω_3 peak induced by unavoidable C substitution effects counteract the possibility of increased T_c in graphene-MgB₂ composites. ω_2 is marginal in G100 and vanishes in G200. ω_3 is gradually shifted to higher frequency in low graphene content samples because the tensile strain has confined the lattice shrinkage. The tensile strain cannot counteract the intensive carbon substitution effects when the graphene content is higher than 10 wt%, and ω_3 takes the place of ω_2 [4]. It should be noted that ω_4 is the strongest peak, as in the other types of carbonaceous chemical doped MgB₂, due to lattice distortion [4]. Furthermore, another peak, ω_5 , has to be considered in G100 and G200 to fit the spectra reasonably well.

Since the E_{2g} mode is considered to be the most relevant phonon in the superconducting transition, the great increases in Γ_2 and Γ_3 are related to the T_c improvement, as well as the frequency. The variations of Γ_2 and Γ_3 for different samples are attributed to the competition between ω_2 and ω_3 due to strain effects and C substitution, as well as the competition between E_{2g} and other modes. The contributions of ω_2 and ω_3 to the strength of EPC(λ), where λ is the electron-phonon coupling constant, can be estimated by the Allen equations, $\Gamma_2 = 2\pi\lambda_2 N(E_F)\omega_2^2$ and $\Gamma_3 = 2\pi\lambda_3 N(E_F)\omega_3^2$, respectively [18, 21], where Γ_2 and Γ_3 represents the FWHM of ω_2 and ω_3 , respectively, in the Raman spectra and $N(E_F)$ is the density of states (per spin per unit energy per unit cell) on the Fermi-surface. The $N_\sigma(E_F)$ and $N_\pi(E_F)$ dependences on T_c were

deduced from the results in the literature [22], as shown in the inset of Fig. 5, and $N(E_F) = [N_\sigma(E_F) + N_\pi(E_F)]/2$ because only one spin was considered in the estimation [16, 23]. The estimated values of λ_2 and λ_3 are plotted in Fig. 5. Consistent with the decay of ω_2 , λ_2 decreases from 2.41 in G000 to 0.92 in G100, which is attributed to the narrowed Γ_2 . λ_3 increases from 0.65 in G005 to 1.36 in G100 before it drops to 0.81 in G200. Although the tensile strain should be more significant in the high graphene content samples due to the increased contact area between the graphene and the MgB_2 , the effect of tensile strain on the superconductivity is counteracted by the carbon substitution, which introduces chemical pressure due to lattice shrinkage. Furthermore, the impurity scattering effects of residual graphene, MgB_2C_2 , and MgO become significant in low T_c samples.

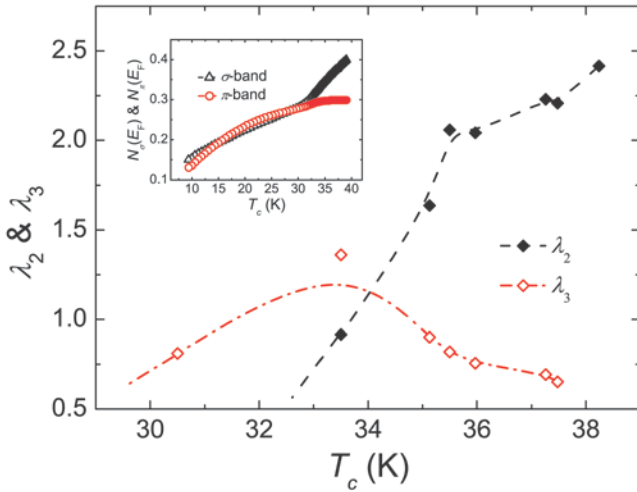


Fig. 5. Electron-phonon coupling constants λ_2 and λ_3 for ω_2 and ω_3 calculated as a function of T_c according to the Allen equation. The inset shows the calculated densities of states at the Fermi energy for the σ - and π -band, $N_\sigma(E_F)$ and $N_\pi(E_F)$, as a function of T_c [22].

IV. CONCLUSIONS

In summary, tensile strain, which increases the EPC strength of MgB_2 , was unambiguously detected in graphene- MgB_2 composites made by the diffusion process. The bond-stretching E_{2g} phonon mode splits into a softened mode due to the tensile strain and another hardened mode due to the carbon substitution on boron sites. Up to 5 wt% of graphene addition is recommended to improve the superconductivity of MgB_2 . Higher T_c values are expected in graphene- MgB_2 composites processed using optimized techniques or doped with stabilized high purity graphene to avoid C substitution.

ACKNOWLEDGMENT

The authors thank Dr. T. Silver for fruitful discussions and helpful critical reading of the manuscript. We acknowledge Dr J. Stride for providing the graphene.

REFERENCES

- [1] J. Nagamatsu, N. Nakagawa, T. Muranaka, Y. Zenitani, and J. Akimitsu, "Superconductivity at 39 K in magnesium diboride," *Nature*, vol. 410, no. 6824, pp. 63-64, Mar 1, 2001.
- [2] S. L. Bud'ko, G. Lapertot, C. Petrovic, C. E. Cunningham, N. Anderson, and P. C. Canfield, "Boron isotope effect in superconducting MgB_2 ," *Physical Review Letters*, vol. 86, no. 9, pp. 1877-1880, Feb 26, 2001.
- [3] K. P. Bohnen, R. Heid, and B. Renker, "Phonon dispersion and electron-phonon coupling in MgB_2 and AlB_2 ," *Physical Review Letters*, vol. 86, no. 25, pp. 5771-5774, Jun 18, 2001.
- [4] W. X. Li, Y. Li, R. H. Chen, R. Zeng, S. X. Dou, M. Y. Zhu, and H. M. Jin, "Raman study of element doping effects on the superconductivity of MgB_2 ," *Physical Review B*, vol. 77, no. 9, pp. 094517, Mar, 2008.
- [5] A. V. Pogrebnnyakov, J. M. Redwing, S. Raghavan, V. Vaithyanathan, D. G. Schlom, S. Y. Xu, Q. Li, D. A. Tenne, A. Soukiassian, X. X. Xi, M. D. Johannes, D. Kasinathan, W. E. Pickett, J. S. Wu, and J. C. H. Spence, "Enhancement of the superconducting transition temperature of MgB_2 by a strain-induced bond-stretching mode softening," *Physical Review Letters*, vol. 93, no. 14, pp. 147006, Oct, 2004.
- [6] J. C. Zheng, and Y. M. Zhu, "Searching for a higher superconducting transition temperature in strained MgB_2 ," *Physical Review B*, vol. 73, no. 2, pp. 024509, Jan, 2006.
- [7] X. Xu, S. X. Dou, X. L. Wang, J. H. Kim, J. A. Stride, M. Choucair, W. K. Yeoh, R. K. Zheng, and S. P. Ringer, "Graphene doping to enhance the flux pinning and supercurrent carrying ability of a magnesium diboride superconductor," *Superconductor Science and Technology*, vol. 23, no. 8, pp. 085003, Jun 29, 2010.
- [8] P. Zhang, S. Saito, S. G. Louie, and M. L. Cohen, "Theory of the electronic structure of alternating MgB_2 and graphene layered structures," *Physical Review B*, vol. 77, no. 5, pp. 052501, Feb, 2008.
- [9] S. M. Kazakov, R. Puzniak, K. Rogacki, A. V. Mironov, N. D. Zhigadlo, J. Jun, C. Soltmann, B. Batlogg, and J. Karpinski, "Carbon substitution in MgB_2 single crystals: Structural and superconducting properties," *Physical Review B*, vol. 71, no. 2, pp. 024533, Jan, 2005.
- [10] S. Lee, T. Masui, A. Yamamoto, H. Uchiyama, and S. Tajima, "Carbon-substituted MgB_2 single crystals," *Physica C-Superconductivity and Its Applications*, vol. 397, no. 1-2, pp. 7-13, Oct 1, 2003.
- [11] T. Masui, S. Lee, and S. Tajima, "Carbon-substitution effect on the electronic properties of MgB_2 single crystals," *Physical Review B*, vol. 70, no. 2, pp. 024504, Jul, 2004.
- [12] W. X. Li, Y. Li, R. H. Chen, W. K. Yeoh, and S. X. Dou, "Effect of magnetic field processing on the microstructure of carbon nanotubes doped MgB_2 ," *Physica C-Superconductivity and Its Applications*, vol. 460, pp. 570-571, Sep 1, 2007.
- [13] R. H. Chen, M. Y. Zhu, Y. Li, W. X. Li, H. M. Jin, and S. X. Dou, "Effect of pulsed magnetic field on critical current in carbon-nanotube-doped MgB_2 wires," *Acta Physica Sinica*, vol. 55, no. 9, pp. 4878-4882, Sep, 2006.
- [14] W. X. Li, Y. Li, R. H. Chen, R. Zeng, L. Lu, Y. Zhang, M. Tomsic, M. Rindfleisch, and S. X. Dou, "Increased Superconductivity for CNT Doped MgB_2 Sintered in 5T Pulsed Magnetic Field," *IEEE Transactions on Applied Superconductivity*, vol. 19, no. 3, pp. 2752-2755, 2009.
- [15] W. K. Yeoh, R. K. Zheng, S. P. Ringer, W. X. Li, X. Xu, S. X. Dou, S. K. Chen, and J. L. MacManus-Driscoll, "Evaluation of carbon incorporation and strain of doped MgB_2 superconductor by Raman spectroscopy," *Scripta Materialia*, vol. 64, no. 4, pp. 323-326, 2011.
- [16] W. X. Li, R. Zeng, L. Lu, Y. Li, and S. X. Dou, "The combined influence of connectivity and disorder on J_c and T_c performances in Mg_2B_3+10 wt % SiC," *Journal of Applied Physics*, vol. 106, no. 9, pp. 093906, Nov, 2009.
- [17] W. X. Li, R. Zeng, C. K. Poh, Y. Li, and S. X. Dou, "Magnetic scattering effects in two-band superconductor: the ferromagnetic dopants in MgB_2 ," *Journal of Physics-Condensed Matter*, vol. 22, no. 13, pp. 135701, Apr, 2010.
- [18] P. B. Allen, and R. C. Dynes, "Transition temperature of strong coupled superconductors reanalyzed," *Physical Review B*, vol. 12, no. 3, pp. 905-922, 1975.
- [19] J. M. An, and W. E. Pickett, "Superconductivity of MgB_2 : Covalent bonds driven metallic," *Physical Review Letters*, vol. 86, no. 19, pp. 4366-4369, May 7, 2001.
- [20] A. Y. Liu, I. I. Mazin, and J. Kortus, "Beyond Eliashberg superconductivity in MgB_2 : Anharmonicity, two-phonon scattering, and multiple gaps," *Physical Review Letters*, vol. 87, no. 8, pp. 087005, Aug 20, 2001.
- [21] W. X. Li, R. Zeng, L. Lu, and S. X. Dou, "Effect of thermal strain on J_c and T_c in high density nano-SiC doped MgB_2 ," *Journal of Applied Physics*, vol. 109, no. 7, pp. 07E108, Apr, 2011.
- [22] G. A. Ummarino, D. Daghero, R. S. Gonnelli, and A. H. Moudden, "Carbon substitutions in MgB_2 within the two-band Eliashberg theory," *Physical Review B*, vol. 71, no. 13, pp. 134511, Apr, 2005.
- [23] W. X. Li, Y. Li, R. H. Chen, R. Zeng, M. Y. Zhu, H. M. Jin, and S. X. Dou, "Electron-phonon coupling properties in MgB_2 observed by Raman scattering," *Journal of Physics-Condensed Matter*, vol. 20, no. 25, pp. 255235, 2008.